

4 DESIGN AND CONSTRUCTION OF RESISTIVE INDUCTORS

The design and construction of the resistive inductors comprised the following steps:

- Quantifying stray resistance and stray inductance in the impulse generator;
- Design approach;
- Resistive inductor construction and verification.

4.1 Quantifying Stray Resistance and Stray Inductance

Consider the lightning impulse combination generator available at the University of the Witwatersrand, configured in current mode as per Figure 3.1. Ideally the resistive inductor component is represented by R_m and L_r , as calculated per waveform and capacitor configuration in Chapter 3. In reality the current impulse generator contains stray resistance, as well as stray inductance due to the physical proximity of the various components e.g. busbars, and the physical internal geometry of the capacitors comprising C_c .

Therefore to achieve a particular waveform, R_m and L_r must take into account the equivalent RLC circuit stray resistance and stray inductance – these include the resistance and inductance presented by the shunt replacing the DUT, as the waveform parameters are defined under short-circuit conditions. Hence:

$$R_m = R_{stray} + R \quad (4.1)$$

$$L_r = L_{stray} + L \quad (4.2)$$

where R is the required resistance (Ω) and L is the required inductance (μH) of the resistive inductors.

Quantifying R_{stray} and L_{stray} per capacitor configuration allows resistive inductors of the correct values to be designed and constructed such that the waveforms are consistent over the three current ranges per C_c .

To quantify R_{stray} and L_{stray} for each capacitor configuration, the generator was set up for short-circuit conditions, a shunt¹ ($R_{shunt} = 0.001 \ \Omega$; $L_{shunt} = 0.15 \ \mu\text{H}$) was placed between the resistive inductor terminals, and $i(t)$ recorded for two or three V_s values. The low R_{shunt} value results in a severely under-damped system, allowing calculation of the 2nd-order system parameters (α and ω_n) and hence system resistance and inductance i.e. R_{sys} and L_{sys} , through a few convenient measurements on the waveform (refer to Appendix B for the measurement method). Then R_{stray} and L_{stray} are simply calculated as follows:

$$R_{stray} = R_{sys} - R_{shunt} \quad (4.3)$$

$$L_{stray} = L_{sys} - L_{shunt} \quad (4.4)$$

From the results it was apparent that a dependency on V_s (or I) existed. Therefore a thorough quantification over as much of the V_s range as was possible - without over-stressing the solenoid-controlled spark gap - was conducted per capacitor configuration².

The results (refer to Appendix C) clearly show downward trends in R_{stray} and L_{stray} for increasing V_s (or I) in all cases. In the calculation, C_c is assumed to be constant but may well vary with V_s - on the other hand $1/\alpha$ is not dependent on C_c , but shows more significant change compared to $1/\omega_n$. In the absence of a full understanding of the effect and hence a more rigorous method, the trend-line R_{stray} and L_{stray} values corresponding to the mid-scale value (or median) of the prospective V_s range were selected per capacitor configuration – refer to Table 4.1.

¹ Measured using a Philips PM6303 RCL meter.

² An additional capacitor configuration later required, comprised three capacitors in parallel (102.3 μF).

Table 4.1: Selection of R_{stray} and L_{stray} per C_c

C_c (μF)	R_{stray} (Ω)	L_{stray} (μH)
8.47	0.063	3.15
33.93	0.018	1.58
136.0	0.007	1.26

Therefore from Table 3.2 and equations (4.1) and (4.2), the required values for R and L , per waveform and capacitor configuration, are shown in Table 4.2, where a 15% tolerance³ on R_m and L_r has been assumed.

Table 4.2: Calculated R and L for each waveform per available C_c

WAVE-FORM	C_c (μF)	LOWER		NOMINAL		UPPER	
		R (Ω)	L (μH)	R (Ω)	L (μH)	R (Ω)	L (μH)
8/20 μs	8.47	0.506	3.1	0.607	4.2	0.707	5.3
	33.93	0.124	0.0	0.149	0.3	0.174	0.5
	136.0	0.028	-0.9	0.035	-0.8	0.041	-0.7
4/40 μs	8.47	4.604	5.7	5.428	7.3	6.251	8.8
	33.93	1.147	0.6	1.353	1.0	1.558	1.4
	136.0	0.284	-0.7	0.335	-0.6	0.386	-0.5
4/55 μs	8.47	6.683	9.0	7.874	11.1	9.064	13.3
	33.93	1.666	1.5	1.963	2.0	2.260	2.5
	136.0	0.413	-0.5	0.487	-0.4	0.561	-0.2
4/70 μs	8.47	8.897	12.5	10.479	15.3	12.060	18.1
	33.93	2.219	2.3	2.613	3.0	3.008	3.7
	136.0	0.551	-0.3	0.650	-0.1	0.748	0.1

Of note are the negative inductance values associated with the 136.0 μF parallel capacitor configuration. These indicate that $L_{stray} > L_r$ such that the associated components must be resistive only i.e. $L = 0 \mu\text{H}$, and that the resultant waveforms will inevitably be longer with an associated decrease in I_{max} (refer to Figure 3.3).

³ Calculations/simulations show that this is acceptable i.e. deviations from the intended waveforms are small.

4.2 Design Approach

Over past years, students have constructed various resistive inductors for the combination generator using multiple strands of Nichrome (resistance) wire and various winding techniques - from solenoids to inductance-reducing windings. Each of these was measured but did not meet the requirements as per Table 4.2. Hence 12 resistive inductors needed to be designed and constructed.

A bundle of Nichrome resistance wire strands is depicted in Figure 4.1.

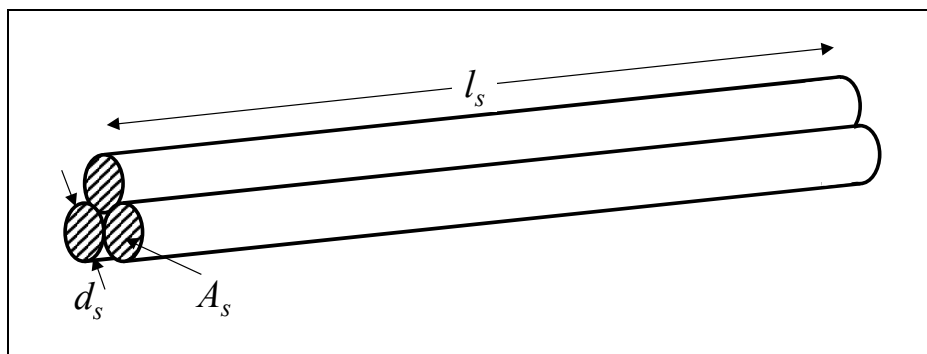


Figure 4.1: Bundle of resistance wire strands

4.2.1 Resistance R

The resistance R of this bundle is:

$$R = \rho \frac{l_s}{s A_s} = R' \frac{l_s}{s} \quad (4.5)$$

where ρ is the Nichrome material resistivity ($\Omega \cdot \text{m}$), l_s is the strand length (m), A_s is the strand cross-sectional area (m^2), s is the number of strands, and R' is the strand ⁴resistance per unit length (Ω/m). Table 4.3 shows reel data for the available⁵ Nichrome wire, where d_s is the strand diameter (mm). Also shown are the calculated ρ values per reel as per equation (4.5) – these typically lie around $0.5 \mu\Omega \cdot \text{m}$ and $1.1 \mu\Omega \cdot \text{m}$ i.e. depends on the constituent proportions of each alloy.

⁴ Resistance wire is typically quoted in resistance per unit length and wire diameter.

⁵ Electrical Engineering Department Workshop, University of the Witwatersrand.

Table 4.3: Available Nichrome wire

REEL	d_s (mm)	R' (Ω/m)	ρ ($\mu\Omega.m$)
1	1.1	0.51	0.485
2	0.914	0.714	0.468
3	0.9	0.79	0.503
4	1.219	0.924	1.078
5	0.813	0.947	0.492
6	1.219	0.98	1.144
7	0.71	1.292	0.512
8	0.914	1.68	1.102
9	0.56	2.004	0.494
10	0.45	3.187	0.507
11	0.4	3.95	0.496
12	0.315	14.1	1.099
13	0.213	14.39	0.513
14	0.193	36.5	1.068

Resistance R is well defined by equation (4.5) and hence easily achieved through appropriate selection of wire from Table 4.3. However thermal capability of the component may not be ignored:

Thermal capability

Referring to Figure 3.1, closure of spark gap S will result in the energy stored in capacitor C_c dissipating as heat energy in R_m under short-circuit conditions. The worst case occurs for $V_{s,max}$:

$$\frac{1}{2}C_c V_{s,max}^2 = mc\Delta T_{max} \quad (4.6)$$

where m is the mass (kg), c is the heat capacity (J/kg. $^{\circ}$ C) and ΔT_{max} is the maximum temperature change ($^{\circ}$ C) of the component. Therefore, if the component⁶ mass is insufficient, its temperature will rise dramatically, thereby affecting its resistance - at worst it will vapourise. The corresponding maximum change in resistance is expressed⁷ as:

⁶ In reality this heat energy is also dissipated in R_{stray} , but $R \gg R_{stray}$.

⁷ Linear approximation holds provided the temperature change is not too great (Giancoli, 1984).

$$\Delta R_{\max} = R_0 \alpha_T \Delta T_{\max} \quad (4.7)$$

where R_0 is the resistance (Ω) at ambient (room) temperature and α_T is the temperature coefficient ($^{\circ}\text{C}^{-1}$).

Assuming $\Delta R / R_0 \leq 5\%$, Table 5.4 shows the resultant ΔT_{\max} and hence the required (minimum) component mass for Nichrome, as well as various other metal conductors, per capacitor configuration.

Table 4.4: Required (minimum) component mass for various conductors⁸ per C_c

C_c (μF)	$V_{s,\max}$ (kV)	NICHROME		ALUMINIUM		COPPER		IRON	
		ΔT_{\max} ($^{\circ}\text{C}$)	m (kg)						
8.47	20	125.0	0.030	11.7	0.161	7.4	0.591	7.7	0.490
33.93	20		0.121		0.647		2.366		1.963
136.0	10		0.121		0.648		2.371		1.967

From Table 4.4 it is evident that Nichrome tolerates a much higher change in temperature, and hence the component mass can be much smaller (up to 17 times) than for the other conductors.

4.2.2 Inductance L

The inductance L of the same bundle of resistance wire strands (Figure 4.1) increases with strand length i.e. larger loop area. From Table 4.2 it is evident that (in general) the high inductance values are associated with high resistance values and *vice versa*. Variation in inductance is achieved through winding geometry i.e. solenoid (for high inductance) or inductance-reducing (for low inductance):

⁸ Nichrome: $\alpha_T = 0.0004 \text{ }^{\circ}\text{C}^{-1}$ (Giancoli, 1984); $c \approx 447 \text{ J/kg}\cdot^{\circ}\text{C}$ i.e. assumed average of Iron (450), Nickel (444) and Chrome (449) (Counterman, 1997a);
Aluminium: $\alpha_T = 0.00429 \text{ }^{\circ}\text{C}^{-1}$; $c = 900 \text{ J/kg}\cdot^{\circ}\text{C}$ (Giancoli, 1984);
Copper: $\alpha_T = 0.0068 \text{ }^{\circ}\text{C}^{-1}$; $c = 390 \text{ J/kg}\cdot^{\circ}\text{C}$ (Giancoli, 1984);
Iron: $\alpha_T = 0.00651 \text{ }^{\circ}\text{C}^{-1}$; $c = 450 \text{ J/kg}\cdot^{\circ}\text{C}$ (Giancoli, 1984).

Solenoid

For a closely packed, air-filled solenoid (long coil), the inductance is described by:

$$L = \frac{\mu_0 N^2 A}{l} \quad (4.8)$$

where $\mu_0 = 4\pi \times 10^{-7}$ T.m/A is the permeability of air, N is the number of turns, A is the solenoid cross-sectional area (m²) and l is the solenoid length (m).

Example: Using Nichrome wire with $d_s = 1$ mm and $l_s = 5$ m, wound (closely packed) on a former of 10 mm diameter, then $N = 160$ turns and $l = 160$ mm. Therefore $L = 16$ μ H.

This example shows that it is relatively easy to achieve the high inductance values in Table 4.2. To prevent inter-turn voltage breakdown, it is necessary to increase the inter-turn spacing, resulting in lower inductance i.e. providing a means to fine-tune the inductance value.

If higher inductance for the same length of wire is required, the solenoid cross-sectional area may be increased, although equation (4.8) will not be valid if the solenoid length is too short compared to the cross-sectional area. Alternatively, the Nichrome wire solenoid could be supplemented by Copper wire turns, or the number of strands s and strand length l_s may be doubled, tripled etc. thereby retaining the required resistance R as per equation (4.5).

Inductance-reducing winding methods

Melaia (1993) experimented with various inductance-reducing techniques for wire-wound resistors (zig-zag, bifilar and Ayrton-Perry) to construct a high voltage, high power resistor with low inductance. Whilst the bifilar method (see Figure 4.2) provided the lowest inductance, it (especially the first few turns) could not withstand high voltage impulses unless thicker insulation (than 4 kV) was used, which simply increased the inductance due to larger inter-turn spacing.

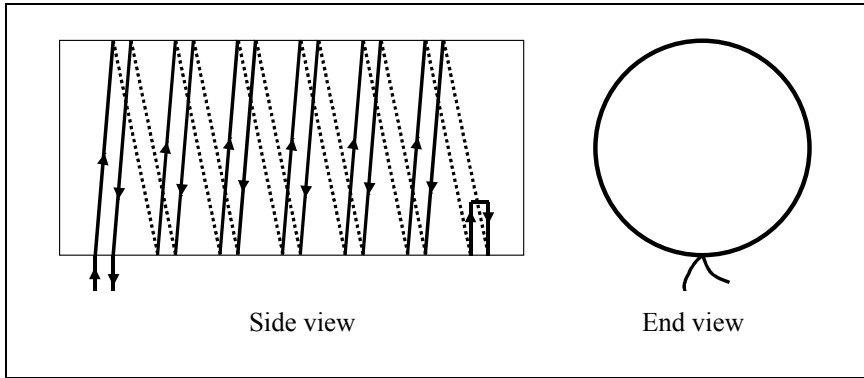


Figure 4.2: Bifilar winding

Finally Melaia realised a method in which the current flow is reversed in adjacent turns, yielding less than half the series inductance of the other techniques, and able to withstand high voltage impulses – refer to Figure 4.3.

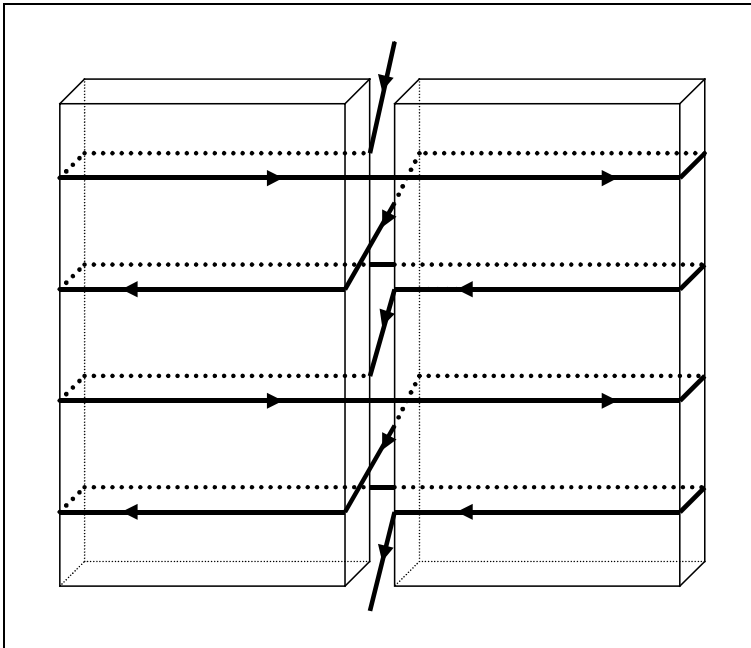


Figure 4.3: Melaia's inductance-reducing method⁹

However in the quest for very low inductance, a winding method – superior to that of Melaia's - was devised in this work, whereby the resistance wire bundle is fashioned into a loop, and every alternate strand loop is twisted through 180° resulting in half the strand loops in anti-parallel. Then the two ends of the set of loops are tightly twisted in opposite directions to reduce the loop area as much as possible – refer to Figure 4.4.

⁹ The turns are shown loosely packed for clarity.

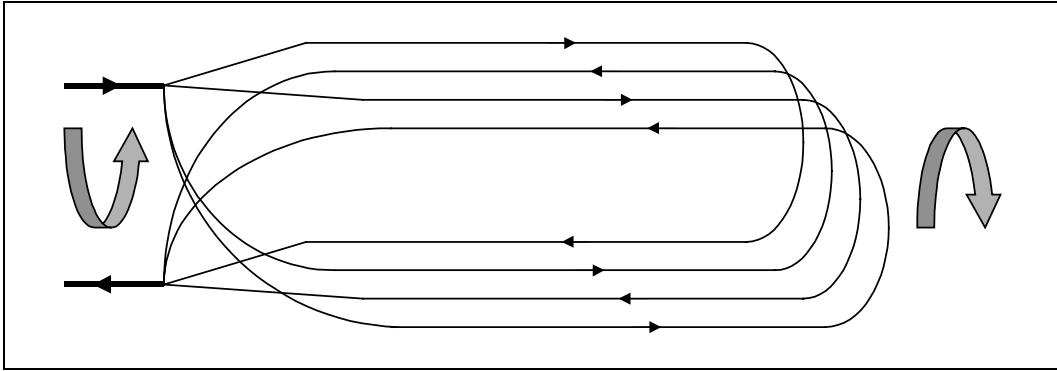


Figure 4.4: Inductance-reducing method – anti-parallel strand loops

The number of strands s must always be even (minimum of 2), and the anti-parallel strand loops must be insulated from the others to withstand high impulse voltage between the two sets – electrical sleeving (braided glass, silicone finish, “proof voltage” of 8 kV) obtained from Wilec¹⁰ fits this purpose.

In comparison to Melaia’s method, a further 30% reduction in inductance is achieved.

Low resistance shunts

For the very low inductance values, low resistance shunts using an alternative conductor e.g. Copper, Aluminium or Iron, could be used. These shunts would typically be thin but broad to keep the inductance as low as possible – refer to Figure 4.5.

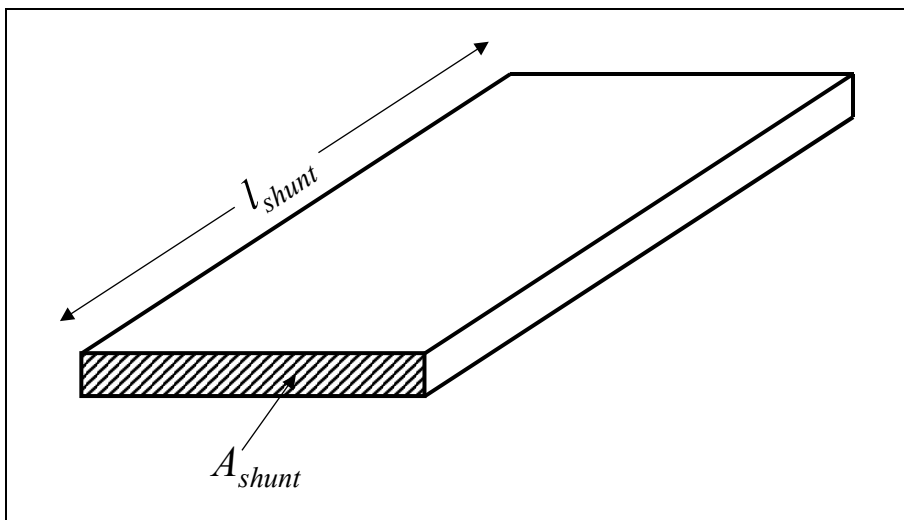


Figure 4.5: Low resistance shunt geometry

¹⁰ Wire Electric (PTY) LTD trading as Wilec.

The resistance R of the shunt is:

$$R = \rho \frac{l_{shunt}}{A_{shunt}} \quad (4.9)$$

where ρ is the conductor material resistivity ($\Omega.m$), l_{shunt} is the shunt length (m), and A_{shunt} is the shunt cross-sectional area (m^2). However cognisance of thermal capability (in Section 4.2.1) essentially dictates the minimum required metal mass m of the shunt:

$$m = P A_{shunt} l_{shunt} \quad (4.10)$$

where P is the conductor density (kg/m^3). Substituting for A_{shunt} in equation (4.9), l_{shunt} is expressed as follows:

$$l_{shunt} = \sqrt{\frac{R m}{\rho P}} \quad (4.11)$$

Table 4.5 shows the required shunt lengths and cross-sectional area for each of the very low inductance components in Table 4.2 based on the required component mass per C_c in Table 4.4.

Table 4.5: Required l_{shunt} and A_{shunt} for various conductors¹¹

R (Ω)	NICHROME		ALUMINIUM		COPPER		IRON	
	l_{shunt} (m)	A_{shunt} (mm^2)						
0.035	0.7 – 1.0	22.1 – 14.9	17.8	13.5	23.6	11.3	9.5	26.5
0.335	2.2 – 3.2	7.1 – 4.8	55.1	4.4	72.9	3.7	29.5	8.6
0.487	2.6 – 3.9	5.9 – 4.0	66.4	3.6	87.9	3.0	35.6	7.1
0.650	3.0 – 4.5	5.1 – 3.5	76.7	3.1	101.5	2.6	41.1	6.1

¹¹ Nichrome: $\rho = 50e-8$ to $110e-8 \Omega.m$ (see Section 4.2.1); $P = 7800 kg/m^3$ i.e. assumed same as Iron (Giancoli, 1984);

Aluminium: $\rho = 2.65e-8 \Omega.m$; $P = 2700 kg/m^3$ (Giancoli, 1984);

Copper: $\rho = 1.68e-8 \Omega.m$; $P = 8900 kg/m^3$ (Giancoli, 1984);

Iron: $\rho = 9.71e-8 \Omega.m$; $P = 7800 kg/m^3$ (Giancoli, 1984).

Clearly Aluminium, Copper and Iron are wholly unsuitable conductors for the purposes of low inductance shunts i.e. l_{shunt} is excessive in all cases. This is due to resistivity ρ that is too low, and a higher component mass m that is required to compensate for relatively high temperature coefficient α_T . Whilst Nichrome is superior in this regard i.e. l_{shunt} is much smaller in all cases, it remains unsuitable for the purposes of low inductance shunts.

Hence for the very low inductance components, it was decided to construct these as short as possible, using Nichrome wire – ensuring that the (thermal) mass requirement in Table 4.4 is met - and achieving an inductance as low as possible using the novel inductance-reducing winding technique (refer to Section 4.2.2). Note that further considerations regarding shunt construction are contained in Appendix D.

4.3 Selecting Optimum s and l_s for Available Nichrome Wire

Consider the bundle of resistance wire strands in Figure 4.1. From equation (4.5):

$$l_s = s \frac{R}{R'} \quad (4.12)$$

where R is the required resistance (Ω), R' is the strand resistance per unit length (Ω/m), l_s is the strand length (m), and s is the number of strands.

Cognisance of thermal capability (refer to Section 4.2.1) essentially dictates the minimum required mass of the bundle. Therefore:

$$m = s P A_s l_s \quad (4.13)$$

where m is the mass of the bundle (kg), P is the Nichrome wire density (kg/m^3) and A_s is the strand cross-sectional area (m^2).

Combining equations (4.12) and (4.13) yields:

$$s = \sqrt{\frac{R' m}{R P A_s}} \quad (4.14)$$

Methodology: Using the appropriate mass value m as per Table 4.4, determine s using equation (4.14) and round up to the nearest integer, for each Nichrome reel per required component. Then calculate l_s for each Nichrome reel using equation (4.12). A few l_s values may emerge for a single s value. The selection of the appropriate Nichrome reel depends on the required inductance:

- For very low inductance, choose l_s as small as possible but ensure s is even-numbered - this is less critical for high s - to enable the novel inductance-reducing winding method to be effective. Avoid very high s , as the individual strands will be too thin and hence unworkable;
- For low to medium inductance, choose small l_s . Typically a heuristic approach (using equivalent length Copper wire strands) is required to investigate the appropriate winding method (e.g. bifilar or very loosely packed solenoid) to achieve the required inductance;
- For high inductance, choose lowest s , then lowest l_s to avoid excessive solenoid length if s and l_s for the selected Nichrome wire need to be doubled, tripled etc.

4.4 Resistive Inductor Construction and Verification

In practice the 8/20 μ s components, as per Table 4.2, were first designed, constructed and verified. As expected (refer to Section 4.1), the third component resulted in a significantly longer waveform, hence a fourth capacitor configuration i.e. three capacitors in parallel (102.3 μ F), was considered. From Appendix C, $R_{stray} = 0.01 \Omega$ and $L_{stray} = 1.28 \mu$ H for $C_c = 102.3 \mu$ F. For the five waveforms, the new R and L requirements - including I_{max} (corresponding to nominal R & L) - are shown in Table 4.6.

Table 4.6: I_{max} , R and L for $C_c = 102.3 \mu\text{F}$

WAVE-FORM	C_c (μF)	I_{max} (kA)	LOWER		NOMINAL		UPPER	
			R (Ω)	L (μH)	R (Ω)	L (μH)	R (Ω)	L (μH)
8/20 μs	102.3	81.2	0.037	-0.8	0.045	-0.7	0.054	-0.6
4/40 μs	102.3	19.9	0.376	-0.5	0.445	-0.4	0.513	-0.3
4/55 μs	102.3	14.1	0.549	-0.3	0.647	-0.1	0.746	0.1
4/70 μs	102.3	10.8	0.732	0.0	0.863	0.2	0.994	0.5

Note: These R and L entries replace the third entry associated with each waveform in Table 4.2.

Compared to $C_c = 136 \mu\text{F}$, I_{max} is reduced by 25%. Furthermore, L remains negative for the first three waveforms; hence the 4/70 μs components were next designed, constructed and verified, as per Table 4.2 (Components 4 and 5) and Table 4.6 (Component 6).

In view of time constraints and extensive effort already expended in the HV laboratory, it was agreed (Geldenhuys, 2001) that no more components were to be designed and constructed, pending creation and analysis of a reduced benchmark sample using the constructed components.

Appendix E details the s and l_s calculations resulting in optimum Nichrome wire selection for the six components. Table 4.7 provides a summary of the parameters for the six constructed components, as well as the resultant R and L .

Table 4.7: Summary of constructed component parameters

COMP.	REEL	s	l_s (mm)	WINDING METHOD ¹²	R (Ω)	L (μH)
1	1	4	4.76	Loosely packed solenoid	0.59	4.0
2	6	10	1.52	Anti-parallel strand loops	0.14	0.3
3	8	37	0.66	Anti-parallel strand loops	0.03	0.2
4	8	1	6.24	Loosely packed solenoid	10.47	14.7
5	8	4	6.22	Loosely packed bifilar	2.60	3.1
6	8	6	3.08	Anti-parallel strand loops	0.87	0.6

¹² Solenoids and bifilar winding on $\varnothing 40$ mm plastic pipes.

These R and L values are well within the lower and upper limits as per Table 4.2 for components 1, 2, 4 and 5 i.e. largest error is 6%. For components 3 and 6, only R is well within the lower and upper limits as per Table 4.2 and 4.6, because the very low inductance requirements proved to be problematic. Nevertheless the novel anti-parallel strand loop method has achieved lower inductance than would otherwise be possible, with the possible exception of low resistance shunts that need to be explored further (refer to Appendix D). Figures 4.6 and 4.7 depict the constructed components, and Table 4.8 (overleaf) shows the resultant circuit parameters (with R_{stray} and L_{stray} as per Table 4.1) and waveform¹³ parameters.

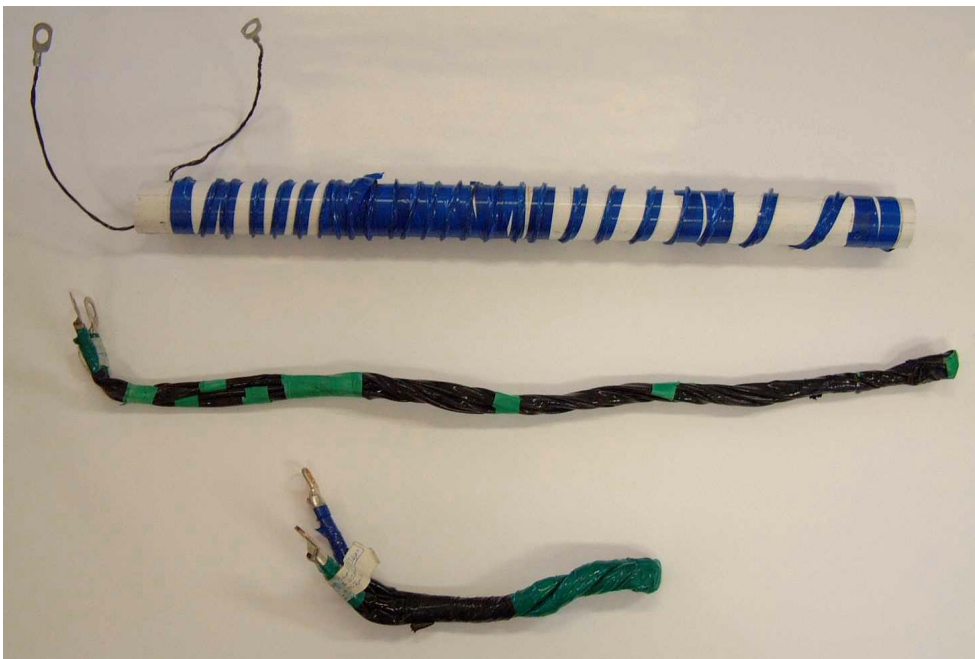


Figure 4.6: Components 1, 2 and 3



Figure 4.7: Components 4, 5 and 6

¹³ T_{front} / T_{tail} obtained via simulations (2nd-order series RLC circuit) in Microsoft® Excel.

Table 4.8: Resultant circuit parameters and waveform per component

COMP.	C_c (μF)	R_m (Ω)	L_r (μH)	$1/\omega_n$ (μs)	$1/\alpha$ (μs)	WAVE-FORM
1	8.47	0.65	7.2	7.8	22.1	8/20 μs
2	33.93	0.16	1.9	8.1	24.3	8/20 μs
3	136.0	0.04	1.5	14.1	78.9	16/36 μs
4	8.47	10.53	17.9	12.3	3.4	4/70 μs
5	33.93	2.62	4.7	12.6	3.6	4/70 μs
6	102.3	0.88	1.9	13.9	4.3	5/72 μs

Cursory inspection of the depicted waveforms (normal view in Figures 4.8 to 4.13) verifies their shape characteristics i.e. T_{front} / T_{tail} as indicated in Table 4.8.

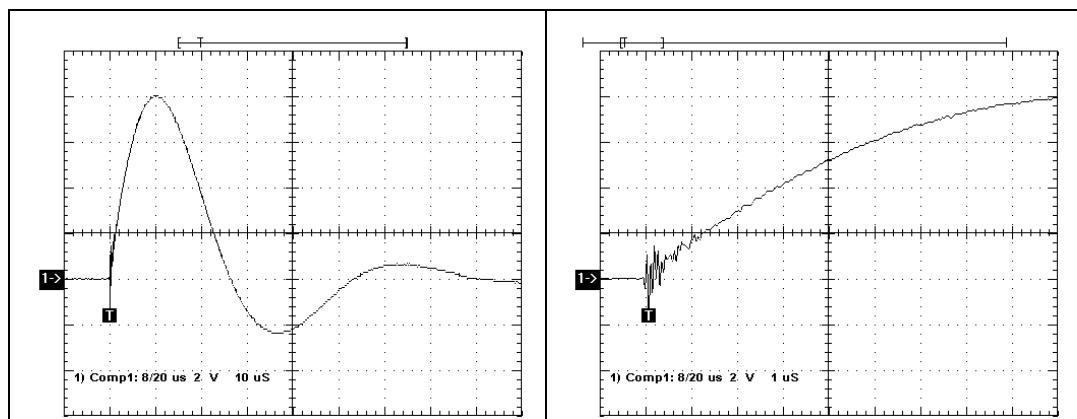


Figure 4.8: Component 1: 8/20 μs waveform (normal and zoomed views)

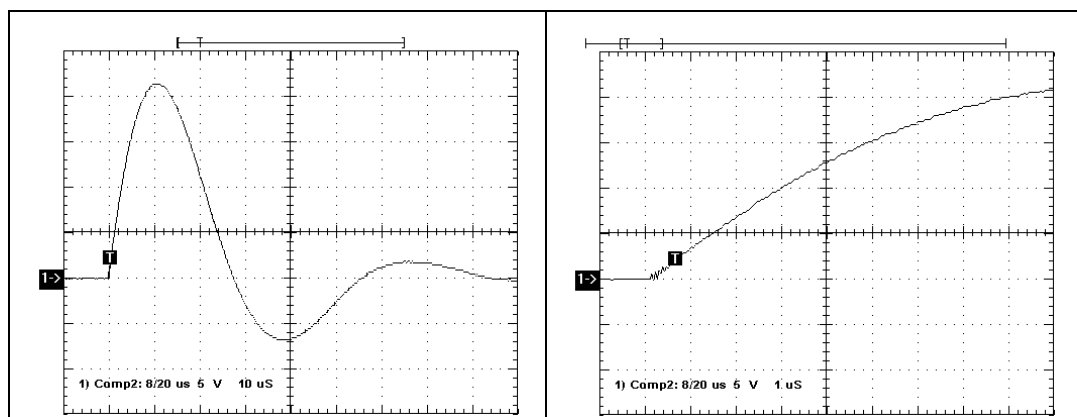


Figure 4.9: Component 2: 8/20 μs waveform (normal and zoomed views)

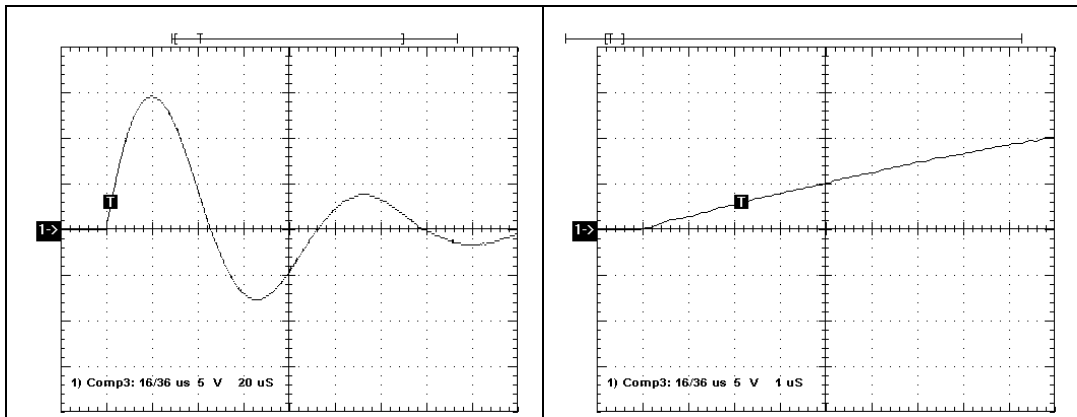


Figure 4.10: Component 3: 16/36 μ s waveform (normal and zoomed views)

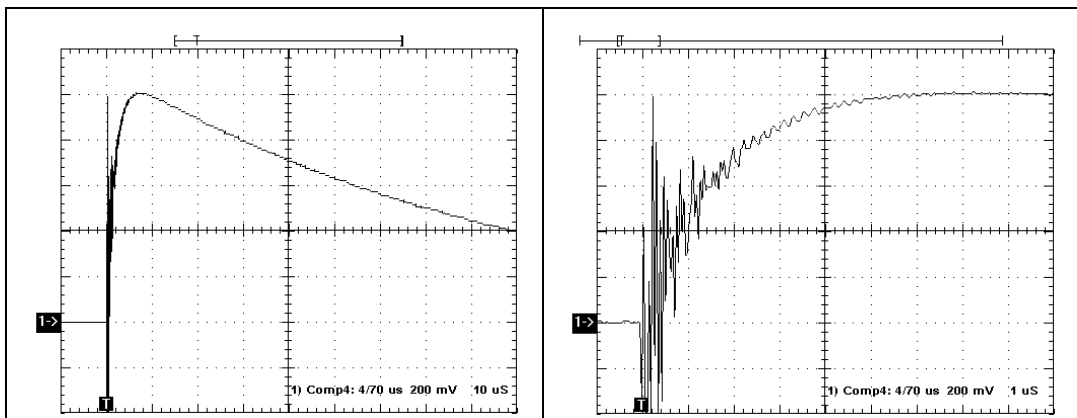


Figure 4.11: Component 4: 4/70 μ s waveform (normal and zoomed views)

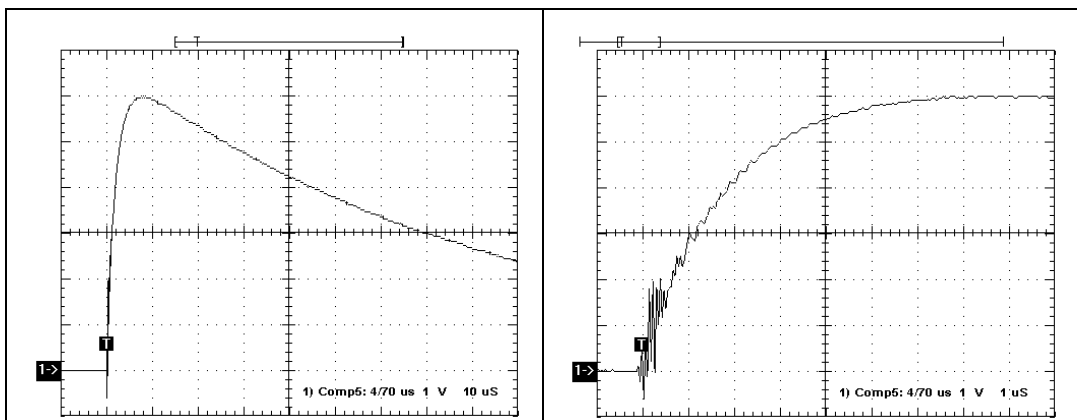


Figure 4.12: Component 5: 4/70 μ s waveform (normal and zoomed views)

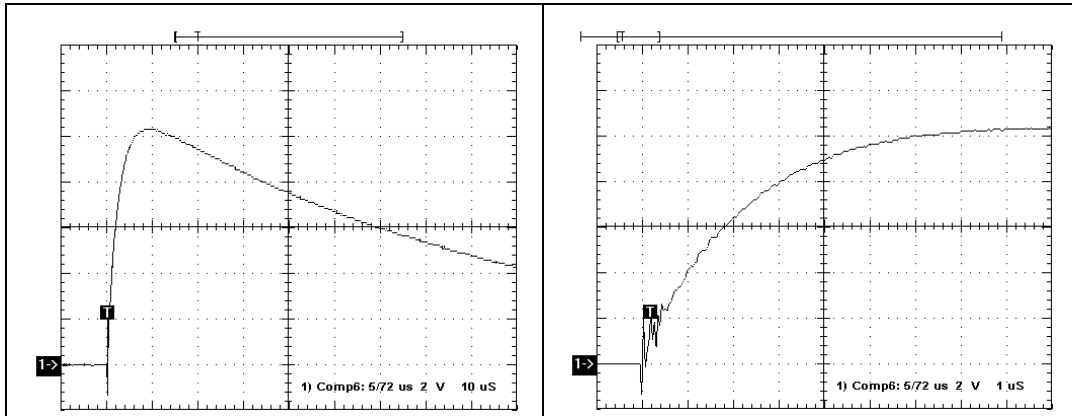


Figure 4.13: Component 6: 5/72 μs waveform (normal and zoomed views)

Zooming in on the origin of each waveform (Figures 4.8 to 4.13 above), ringing is evident for most of these as follows:

- Component 3: None;
- Component 2: Insignificant ringing within 0.5 μs ;
- Component 6: Some ringing within 1 μs ;
- Components 1 and 5: More pronounced ringing within 1 μs and 0.5 μs respectively;
- Component 4: Severe ringing within 2 μs ;

The ringing is most probably due to inter-turn (parasitic) capacitance of the components, which would be least pronounced for the shortest anti-parallel strand loops component i.e. Component 3, and most pronounced for the higher inductance (relatively closely-spaced turns) solenoid i.e. Component 4. For the latter component, a more loosely spaced solenoid would be beneficial but would require longer l_s and hence an excessive solenoid length. The alternative is to insert a core with a relative permeability between 2 and 5 into a relatively short solenoid to increase the inductance i.e. amend the methodology as follows:

- For high inductance, choose lowest s , then lowest l_s , and effect a very loosely packed solenoid onto a low relative permeability core, ensuring that core saturation cannot occur during use.

Alternatively (or additionally) it is possible that magnetic flux, produced by current through the horizontally mounted spark gap of the impulse generator, links directly with the horizontal turns of the solenoid and bifilar components i.e. Components 1, 4 and 5. This would be most pronounced with the higher inductance solenoid i.e. Component 4 and least pronounced with the bifilar component i.e. Component 5. Therefore ringing may be reduced if the spark gap assembly is either magnetically screened or vertically mounted.

4.5 Conclusion

Quantifying stray resistance and inductance proved to be crucial because these represent a significant proportion of the desired values of R_m and L_r . For example, $L_{stray} = 0.88L_r$ for Component 2. Therefore ignoring R_{stray} and L_{stray} would have resulted in significantly differing waveforms from those desired; each of the desired waveforms had to be consistent over the current ranges.

Provided $L \geq 0$, any of the required resistance and inductance values are easily met, where the low inductance components need to be small (short). But thermal capability of the components demands sufficient thermal mass to avoid significant changes in resistance value or at worst destruction of the components. Hence the design and construction of the low inductance components was challenging – during this process a novel inductance-reducing winding technique comprising anti-parallel strand loops was devised - yielding a further 30% reduction in inductance compared to Melaia's method.

For the very low inductance required by some components, it may be possible to use shunts of low thermal mass immersed in a fluid having high heat capacity, but low electrical conductivity – such further considerations are given in Appendix D but would need to be explored further.

Due to time constraints, six components out of the required 12 were constructed to represent the 8/20 μs and 4/70 μs waveforms, pending creation and analysis of a reduced benchmark sample using these components. However due to the stray inductance limitation - particularly demanding for the third capacitor

configuration - Components 3 and 6 yield 16/36 μs and 5/72 μs waveforms respectively. Whilst the latter is a reasonable approximation of a 4/70 μs waveform, the former is unsuitable for further use i.e. creation of a benchmark sample.

For the six components, three different winding techniques were utilised: loosely packed solenoid, loosely packed bifilar and anti-parallel strand loops. The third method produced the smoothest waveforms, whilst the other two produced waveforms with moderate to severe ringing at the origin, most probably due to inter-turn (parasitic) capacitance and/or magnetic flux linkage between the horizontally mounted spark gap and the horizontal turns of the components. Therefore it is recommended that the spark gap assembly is magnetically screened and/or vertically mounted.